Nanoarchitectonics
http://ojs.wiserpub.com/index.php/NAT/

UNIVERSAL WISER
PUBLISHER

Research Article

Synthesis and Applications of Processable Prussian Blue Nanoparticles

Prem C. Pandey*, **Priyanshi Pandey**

Department of Chemistry, Indian Institute of Technology, Banaras Hindu University, Varanasi-221005, India
Email: pcpandey.apc@iitbhu.ac.in

Received: 27 May 2020; **Revised:** 30 June 2020; **Accepted:** 9 July 2020

Abstract: The present report describes a comparative study on chemical synthesis of processable Prussian blue Nanoparticles (PBNPs) suitable for developing PB-based devices. Controlled nucleation of PBNP from single precursors, Potassium hexacyanoferrate, has been recorded as a function of reducing and stabilizing ability of some active organic reducing agents. The use of organic reagent control the nucleation process yielding PBNPs displaying both homogeneous and heterogeneous catalysis. Four different systems of active organic reducing agents i.e.: (1) 3-aminopropyltrimethoxysilane (3-APTMS) and cyclohexanone, (2) tetrahydrofuran hydroperoxide, (3) tetrahydrofuran and hydrogen peroxide and (4) tetrahydrofuran hydroperoxide and 2-(3, 4-epoxycyclohexyl) ethyltrimethoxysilane resulted the formation of $PBNP_1$, $PBNP_2$, $PBNP_3$ and $PBNP_4$ displaying *sensitivity of analysis to the order of* 480, 330 350 and 400 $\mu A\ mM^{-1}\ cm^{-2}$ respectively. The as reported process also enable the controlled synthesis of noble metal nanoparticles introducing new rout for yielding Prussian blue-noble metal nanoparticle nanocomposite that manipulate the catalytic/elecrocatalytic activity for targeted system. As made PBNPs undergo the formation of homogeneous nanodispersion with gold nanoparticles and ruthenium bipyridyl with gradual enhancement in the catalytic activity. The typical application in probing glucose oxidase catalyzed reaction based on both homogeneous and heterogeneous catalysis has been recorded. In addition the synthetic approach could also be explored to incorporate Prussian blue and palladium nanoparticles in mesoporous matrix for developing variety of PB-based devices.

***Keywords*:** PBNPs, H_2O_2, electrocatalytic activity, PdNPs, PBNP-AuNP hybrid, glucose biosensing

1. Introduction

The development of nanomaterial displaying variety of properties typically electrocatalytic ability, magnetic susceptibility, electrochromic and photophysical ability have received closer attention for research and innovation. One of well known synthetic coordination compound, Prussian blue (PB), commonly referred as metal hexacyanoferrate, simultaneously display these properties [1-16]. The presence of iron in two oxidation states allows the resemblance of PB with peroxidase enzyme being used as label during many clinical applications. The replacement of peroxidase by PB seems to be quite attracting for generating Bioanalytical systems where susceptibility of enzymatic activity to various environmental conditions could be controlled. However, many exciting properties of PB could not be explored for practical application mainly due to non-processability of synthetic materials attributed to uncontrolled nucleation during many conventional synthetic strategies. Accordingly synthetic strategy controlling the nucleation process during PB crystal formation has been an exciting and promising research interest. Such process might yield into the formation of PB nanoparticles that may further be processed into various formulations for specific applications. The

Copyright ©2020 Prem C. Pandey, et al.
DOI: https://doi.org/10.37256/nat.212021443
This is an open-access article distributed under a CC BY license
(Creative Commons Attribution 4.0 International License)
https://creativecommons.org/licenses/by/4.0/

ferrrocyanide/ferricyanide complex ions undergo interaction with ferric/ferrous ions resulting a network of high-spin iron (III) ions bound to the nitrogen of cyanide ions and the low-spin iron(II) ions bridge the high-spin iron (III) and low spin iron (II) ions so effectively resulting in an intense charge transfer generating to the blue color in PB. Accordingly, the synthetic process involves the participation of either double precursors method i.e. potassium ferricyanide and ferric ions or potassium ferricyanide and ferrous ions and or may also be associated with single precursor method i.e. preferably potassium ferricyanide, in the presence of species that allow the dissociation of some fraction of single precursor into ferrous or ferric ions. Double precursors method is conventional and lead to uncontrolled nucleation rendering the practical usability of pigment and has been limited to electrochemical synthesis of PB film on desired electrode surface as efficiently studied by Karykin et al [1-2] covering various combination of transition metal cations yielding electrodeposited Prussian blue and its mixed metal analogues in form of commercial printed electrodes useful in biosensing. Kurihara et al [13-14] studied in details on the processing of the insoluble PB pigment in both non-aqueous and aqueous media and innovated the formation of ideal soluble PBNPs inks for potential applications. Although these methods yielded model PB preparation with subsequent limitation in yielding many PB-based designs. Single precursor method can be easily controlled from the use of organic reagent, thus not requiring any further processing, that is not part of the MHCF network however, allow controlled dissociation of fraction of single precursor, e.g. potassium ferricyanide, into ferrous or ferric ions thus enabling controlled formation of PB nanoparticles (PBNP) followed by stabilizing the as generated PBNPs as given below;

$$K_3Fe(CN)_6 \xrightarrow[\mathbf{H^+}]{\textbf{Organic reducing Agent/}} [Fe(CN)_6]^{3-} + Fe^{3+} \tag{1}$$

$$Fe^{3+} \xrightarrow{\textbf{Organic reducing Agent}} Fe^{2+} \tag{2}$$

$$[Fe(CN)_6]^{3-} + Fe^{2+} \xrightarrow{\textbf{Organic reagent/Stabilizer}} PBNPs \tag{3}$$

Accordingly the choice of such organic reagent is very important that may further affect the processability, electrochemical activity and stability of PBNP for specific applications along with added novelty in manipulating the properties of the same. Further the efficiency of these organic reducing agent may allow variable rate for the formation of dissociation product of Prussian blue precursor followed by conversion of the oxidation state of Prussian blue component which is key point in yielding pigment with better Prussian blue character. Accordingly we have already demonstrated various organic reagents [26-31] to yield PBNPs with further requiring a comparison on the electrochemical activity for further applications.

Several heterostructured systems that combine noble metal nanoparticles with MHCF have been studied because of their enhanced catalytic activity or because of an association of the magnetic or optical properties of the inorganic NPs with the porosity and the electrochemical or magnetic properties of the coordination polymers [17-18]. Among these inorganic cores, gold NPs are particularly appropriate for the design of multifunctional systems owing to their catalytic properties and the optical features that arise from the surface plasmon band and directed us to manipulate the electrocatalytic activity of PBNP in the presence of noble metal nanoparticles (MNP) i.e. gold, silver and palladium through the formation of PBNP-MNP hybrids. Accordingly the choice of organic reagent that not only allow the controlled conversion of single precursor into PBNP but simultaneously also enable the controlled conversion of noble metal cations into respective nanoparticles may have greater impact in the synthesis of functional nanomaterials. We have demonstrated the role of these organic reducing agent during the synthesis of mono-metallic, bimetallic and trimetallic nanoparticles [19-22]. Accordingly, we attempted to make hybrid of PBNP and metal nanoparticles especially AuNP to understand variation in electrocatalytic activity if any for catalytic applications. In addition the processability of the PBNP may further be explored to make homogeneous dispersion of the hybrid with other active molecule like Ruthenium bipyridyl if such incorporation may further manipulate the catalytic properties of PBNP hybrid.

In addition it has been shown that nanocatalysts confined in the interior of porous showed much better catalytic activity and selectivity in comparison with those located outside the matrix associated to unique confinement effect of functional nanoparticles. Such system may allow to design switchable molecular materials [23] that are attractive for the design of multifunctional innovative devices since their physical properties can be tuned by the application of various external stimuli [24] and reveals that the properties of such material can be tuned to desired application within confined mesoporous matrix as compared to that of in unconfined geometry [23-25]. Accordingly, the choice of organic reagent that also allow the confinement of PBNPs within mesoporous matrix along with noble metal nanoparticles may further results into the switchable molecular material of specific applications [26-31]. The present article describe the role of 3-amnopropyltrimethoxysilane, cyclohexanone, tetrahydrofuran hydroperoxide that enable the PBNPs formation as homogeneous suspension of PBNPs, hybrid of PBNP and MNP along with enabling the synthetic incorporation of PBNPs and PdNP within mesoporous matrix and reported in this article.

2. Experimental section

2.1 *Materials*

3-aminopropyltrimethoxysilane, cyclohexanone, 2-(3, 4-epoxycyclohexyl) ethyltrimethoxysilane, glucose oxidase, tetrahydrofuran, Graphite powder (particle Size 1-2 µm), Nujol oil (density 0.838g mL^{-1}) were obtained from Sigma-Aldrich Chemical Co. India. Potassium ferricyanide and hydrogen peroxide (H_2O_2) were purchased from Merck, India all other chemicals used were obtained from the commercial source and were of analytical grade. Double distilled water was used in all experiments.

2.2 *3 -APTMS and cyclohehanone mediated synthesis of $PBNP_1$*

The typical process of PBNPs synthesis is similar to those reported earlier [27]. The process involves mixing of 50 µL aqueous solution of potassium ferricyanide (0.05 M) and 10µL of 3-APTMS (0.5 M) under stirred conditions over a vertex cyclo mixer followed by the addition of 2 µL cyclohexanone (9.62 M) resulting into bright green color and subsequently converted to deep blue PBNPs sol after vigorous stirring. The resulting deep blue PBNPs sol was mixed with 5 µL HCl (6.5 M) under stirred condition. The optimum concentrations of cyclohexanone/potassium ferricyanide/3-APTMS required for best $PBNP_1$ sol formation were achieved by varying the concentrations of one component while keeping fixed concentrations of other two components

2.3 *Tetrahydrofuran hydroperoxide mediated synthesis of $PBNP_2$*

The typical process of $PBNP_2$ synthesis was similar to that described earlier [28]. 50 µL aqueous solution of potassium ferricyanide (0.5 M) and 200 µL of THF-HP was mixed under stirred conditions over a vertex cyclo mixer. The mixture immediately turns into green color which was left to stand for 12 h. After this, the color of the solution turned to blue indicating the formation of $PBNP_2$. The $PBNP_2$ may be treated with ethyl acetate to eliminate residual organic moiety and collected by centrifugation followed by washing and drying.

2.4 *Tetrahydrofuran and hydrogen peroxide mediated synthesis of $PBNP_3$*

The typical process of $PBNP_3$ synthesis was similar to that described earlier [29]. 70 µl aqueous solution of K_3 [Fe $(CN)_6$] (0.05 M) and 10 µl of THF(12 M) were mixed under stirred condition over vertex cyclo-mixture followed by addition of 20µl of H_2O_2 (3.5 M). The resultant mixture was kept at 60°C for 20 minutes in an oven. The yellow colour solution of K_3 [Fe $(CN)_6$] was turned into deep blue colour solution which indicates the formation of $PBNP_3$. $PBNP_3$ may be treated with ethyl acetate to eliminate residual organic moiety and collected by centrifugation and dried the precipitate.

2.5 *2-(3, 4-epoxycyclohexyl) ethyltrimethoxysilane mediated synthesis of $PBNP_4$*

The typical process of $PBNP_4$ synthesis as described earlier [30] that involves the mixing of optimum concentration of 2-(3, 4-epoxycyclohexyl) ethyltrimethoxysilane and an aqueous solution of potassium ferricyanide followed by addition of tetrahydrofuran hydroperoxide (THF-HPO) under stirring condition. The resulting green colored solution was allowed to stand in an oven at 60^oC for 3-5 h to yield deep blue $PBNP_4$ homogeneous suspension and was initially purified by solvent extraction using ethyl acetate.

2.6 *Synthesis of PBNP-PdNP suspension*

Synthesis of PBNP and its nandispersion with PdNP.

The procedure adopted for the synthesis of PBNP-PdNP hybrid is similar to that reported earlier [31]. 50 µL aqueous solution of potassium ferricyanide (0.5 M) was mixed with 200 µL of tetrahydrofuran hydroperoxide (THF-HPO) under stirred conditions and left to stand for 12 h. The colour of the solution turned to blue indicating the formation of PBNP. PdNP were synthesized by mixing an aqueous solution of K_2PdCl_4 (0.003 M, 50 µL) and 10 µL of two different concentrations of 3-APTMS i.e. 0.5 M and 1 M under stirred condition over a cyclo mixer followed by the addition of THF-HPO (15 µL) in each one at room temperature resulting the formation of $PdNP_1$ and $PdNP_2$ respectively. The mixture turns into light black colour within < 15 min which subsequently converted to dark black colour of PdNP sol of different size i.e. $PdNP_1$ and $PdNP_2$ as a function of 3-APTMS concentrations (0.5 M, 1 M). The nanocomposite formation involves the mixing of 100 µl of PBNP and 50 µl of $PdNP_1$ or $PdNP_2$ solutions, leading to the formation of a homogeneous nanodispersion of PBNP-$PdNP_1$ and PBNP-$PdNP_2$ respectively.

2.7 *Tetrahydrofuran hydroperoxide mediated synthetic insertion of Prussian blue and PdNP nanoparticles within mesoporous silica nanoparticles*

200ml aqueous solution of K_2PdCl_4 (0.003 M) was added to 5 mg of mesoporous silica nanoparticles. After addition of 3-APTMS (1 M, 40 µL) the resulting suspension was continuously stirred for 1-2 h at 25°C. The 3-APTMS treated mesoporous silica nanoparticle was collected by centrifugation and washed with methanol. 60 ml tetrahydrofuran hydroperoxide (0.2 M) was then added to the mixture which was allowed to react under constant stirring for 1-4 h at 25°C to yield PdNP inserted Mesoporous nanoparticles. The as made PdNPs within mesoporous silica nanoparticles was collected by centrifugation followed by washing with ethanol for several time to ensure complete removal of any unbound palladium species.

THF-HPO (200 ml) treated Potassium ferricyanide (100 ml, 0.5 M) was then added to PdNP-inserted Mesoporous silica nanoparticle and continuously stirred for 1-2 h at 25°C. After The mixture was incubated at 35°C for 12 h to yield the conversion of potassium ferricyanide into PBNPs within mesoporous silica spheres. PdNP-PBNP inserted mesoporous silica spheres was collected by centrifugation followed by washing with ethanol several times to ensure the removal of any unbound PBNP from Mesoporous nanoparticles. The as formed PdNP-PBNP inserted Mesoporous silica nanoparticle could be dried at 60°C to yield blue coloured powder or to be used as homogeneous suspension.

3-APTMS and organic reducing agents mediated synthesis of AuNP, PdNP and Pd-Au nanoparticles

The procedure for the synthesis of gold nanoparticles using 3-APTMS and cyclohenone/tetrahydrofuran gydroperoxide was similar to that reported earlier [19-22]. These reagents also enable the formation for Pd-Au or AuPd either through simultaneous or sequential mode of metal cation reduction as described earlier [21-22].

Measurements and characterization:

The UV-Vis absorption spectra of PBNPs were recorded using a Hitachi U-2900 Spectrometer. Transmission electron microscopy (TEM) studies were performed using Hitachi 800 and 8100 electron microscopy (Tokyo, Japan) with an acceleration voltage of 200 kV. IR spectra recorded on an ALFA FTIR Bruker-ATR, Ettington, Germany. Electrochemical experiments were accomplished on an Electrochemical workstation Model CHI660B, CH Instrument Inc., TX, in a three-electrode configuration with a working volume of 3 ml. An Ag/AgCl electrode served as reference and counter electrode, respectively. All potentials given in the text are relative to the Ag/AgCl. The working electrode was a PBNPs-modified carbon paste electrode (CPE). The active paste of PBNPs was made by mixing 100 µl of PBNPs suspension with 60 mg spectroscopic grade graphite powder (particle size 1-2 µ), followed by ultrasonication for 30 minutes and left to dry in a vacuum oven overnight. Electrode body used for electrochemical measurement has been purchased from Bioanalytical systems (West Lafayette, In (MF 2010). The composition of the typical active paste was found to be, graphite powder = 68%, w/w, and nujol oil = 28%, w/w, PBNPs = 4% w/w.

3. Result and discussion

3.1 *Role of organic reducing agents in controlled conversion PBNPs*

The finding demonstrated earlier clearly predict the occurrence of uncontrolled nucleation when Prussian blue are made from double precursors unless other wise under specific conditions required to control the nucleation step is adopted [13-14]. Accordingly we demonstrated the role of 4 different organic reagents that enable the controlled conversion [26-31] of single precursors into PBNPs; (i) 3-APTMS and cyclohexanone, (ii) tetrahydrofuran hydroperoxide, (iii) tetrahydrofuran and hydrogen peroxide and (iv) tetrahydrofuran hydroperoxide and 2-(3, 4-epoxycyclohexyl) ethyltrimethoxysilane. These reagents precisely control the nucleation of PBNP due to slow dissociation of fraction of single precursors followed by variation in the oxidation state of as generated iron. Such process is the dissociation and reducing ability of these reagents and allow the formation of four different type of PBNPs namely PBNP$_1$, PBNP$_2$, PBNP$_3$ and PBNP$_4$. Figure 1 show the absorption spectra along with visual photographs of PBNP formation as a function of organic reducing agents. The finding clearly predicts that the absorption at 670 nm is different in all four types of systems. The relatively better PB character is recorded in the system derived from; (a) 3-APTMS and cyclohehexanone and (b) tetrahydrofuran hydroperoxide and 2-(3, 4-epoxycyclohexyl) ethyltrimethoxysilane as evidence from TEM analysis as shown in Figure 2a (I). The average size of PBNP$_1$ and PBNP$_4$ are found to 7-11 nm with 3-APTMS and cyclohexanone and 8-12 nm with tetrahydrofuran hydroperoxide and 2-(3, 4-epoxycyclohexyl) ethyltrimethoxysilane. The other two system i.e. (i) tetrahydrofuran hydroperoxide and (ii) tetrahydrofuran and hydrogen peroxide yielded the formation PBNP$_2$ and PBNP$_3$ having average size to the order of 20-40 nm. Such variation in PBNP properties is mainly the efficiency of organic reagent that allow the dissociation of single precursor that subsequently control the nucleation process. This results variation in polycrystallinity of as made PBNP as shown in Figure 2a (II) justifying the presence of all planes attributed to face centered cubic structure [Figure 2a (II)] of PBA.

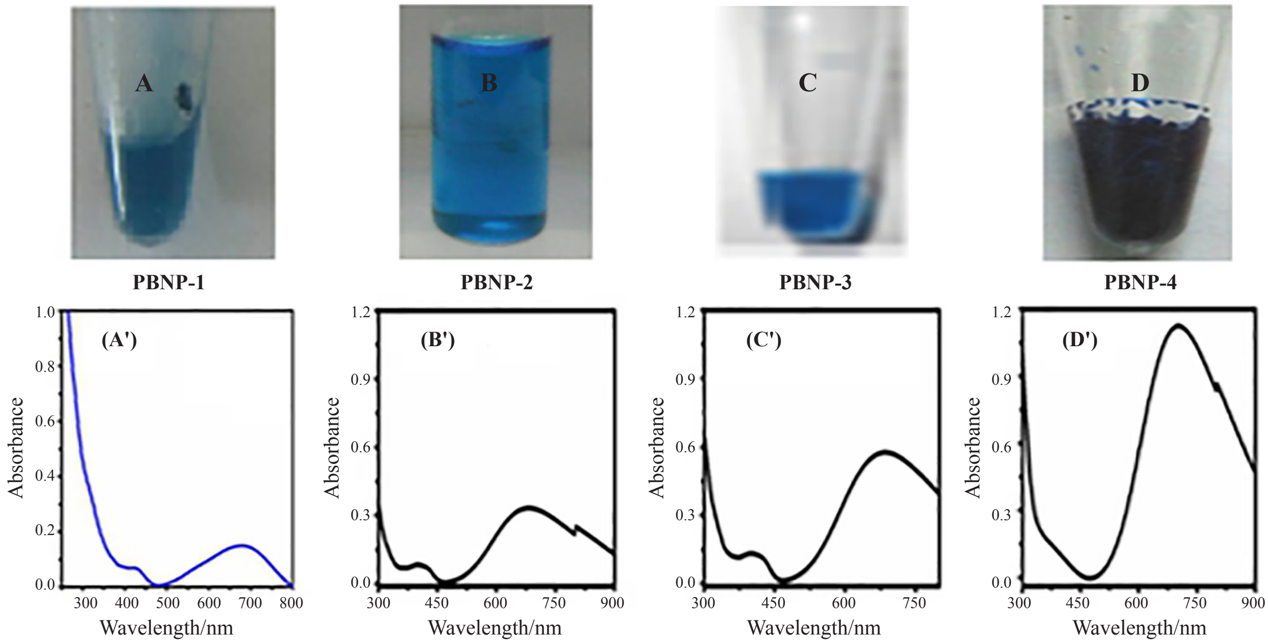

Figure 1. Effect of four different organic reducing systems (i) 3-Aminopropyltrimethoxysilane and cyclohexanone, (ii) tetrahydrofuran hydroperoxide, (iii) tetrahydrofuran and hydrogen peroxide, and (iv). 2-(3, 4-epoxycyclohexyl) ethyltrimethoxysilane and tetrahydrofuran hydroperoxide for the synthesis of PBNP1, PBNP2, PBNP3 and PBNP4; The inset to Figure 1 show the visual images of the respective systems

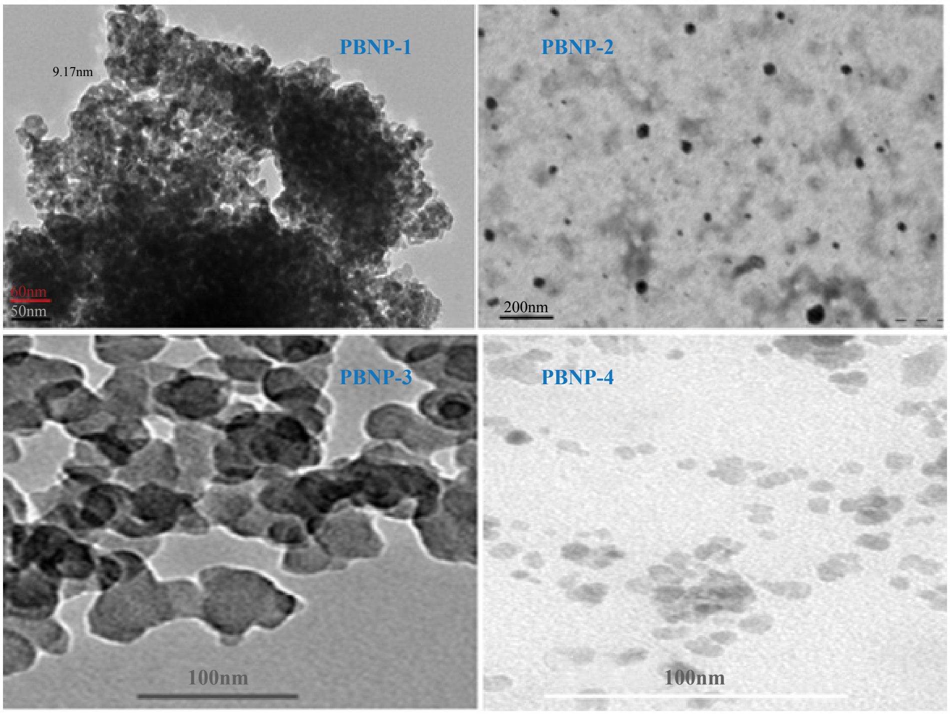

Figure 2a. (I) TEM images of PBNP1. PBNP2, PBNP3 and PBNP4 Nanoparticles

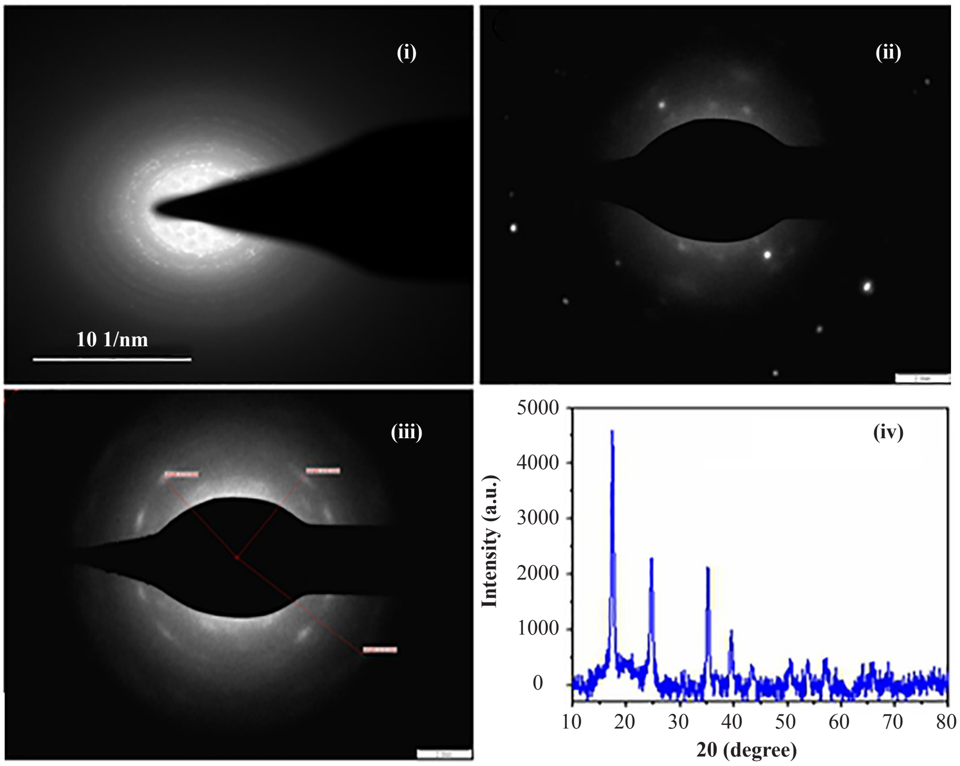

Figure 2a. (II) SAED of PBNPs (i-iii) along with XRD pattern (iv)

These regents also enable the reduction of noble metal cations into respective nanoparticles. It has been demonstrated [19-21] that 3-APTMS capped noble metal cations i.e. Au^{3+}, Ag^{+}, and Pd^{++} undergo control conversion into AuNPs, AgNPs and PdNPs. In addition bimetallic and trimetallic nanoparticles are also efficiently made through the participation of the these organic reagents [23, 32], in the presence of 3-APTMS. Figure 2b shows the TEM images of as made AuNPs, PdNPs and bimetallic Pd-Au nanoparticles. It is also possible to control the morphology and dispersibility of these metal nanoparticles in different solvent as per requirement based on the choice of 3-APTMS-tetrahydrofuran hydroperoxide or 3-APTMS and cyclohexanone. The use of similar reagent in yielding both PBNPs and metal nanoparticles also facilitated in the formation of nanodispersion of metal nanoparticles embedded PBNP hybrids. Figure 3a shows the TEM images of PBNP-PdNP and PBNP-AgNP hybrids. Similarly Figure 3b shows the HR SEM images of PBNP and PBNP-PdNPs derived from similar organic reagents. These finding clearly predicts the valuable contribution in yielding the PBNPs of desired size that further enable the formation of PBNP and metal nanoparticles hybrids in order to manipulate the catalytic activity of PBNPs which is one most wanted requirement in catalytic science and technology.

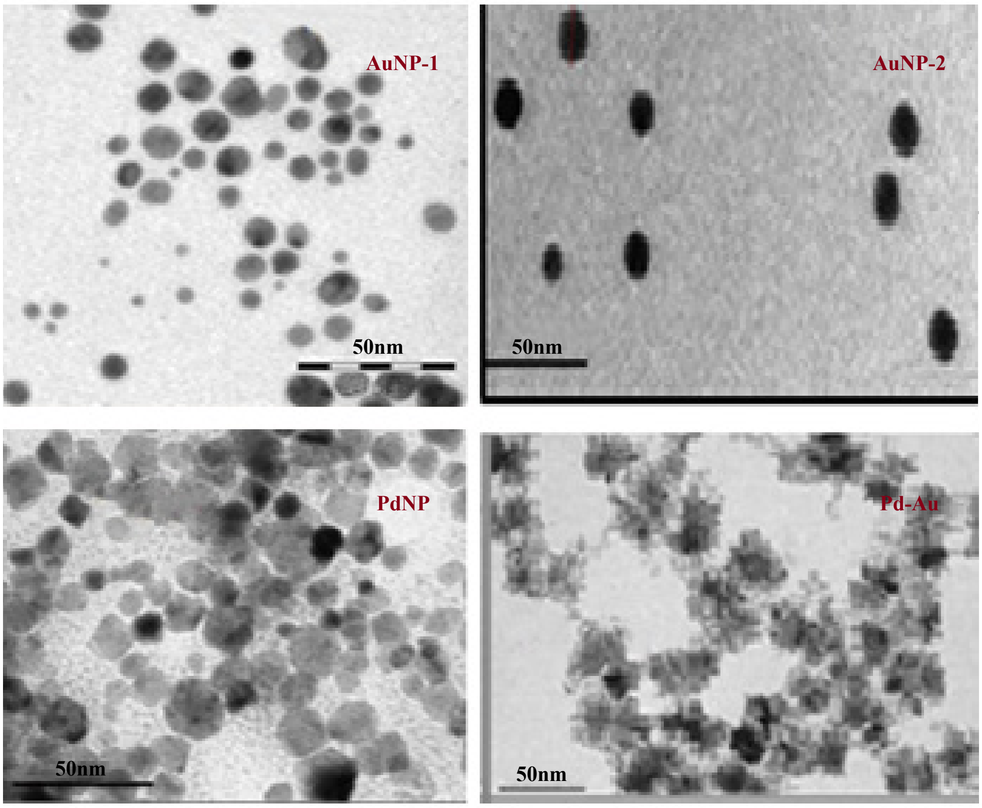

Figure 2b. TEM images; AuNP1 and AuNP2 made from 3-APTMS and cyclohexanone and 3-APTMS and tetrahydrofuranhydroperoxide; PdNP and Au-PdNP made from 3-APTMS and tetrahydrofuran hydroperoxide

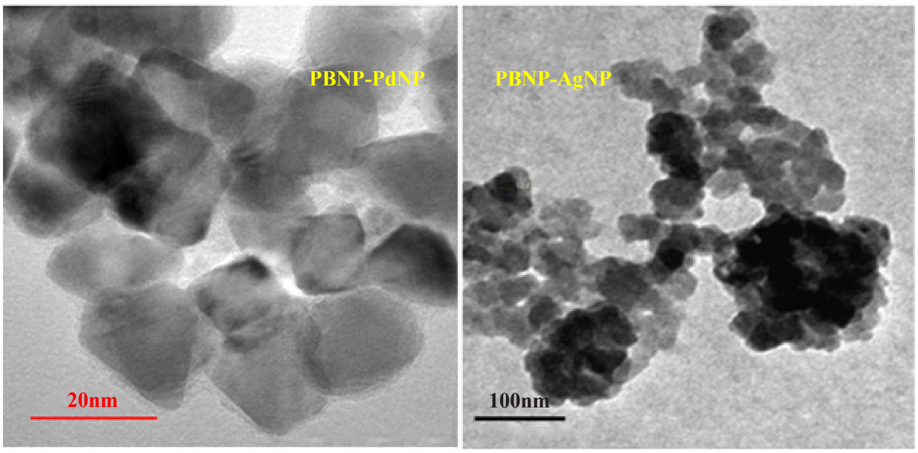

Figure 3a. PBNP-PdNP hybrid made from 3-APTMS and tetrahydrofuran hydroperoxide; PBNP-AgNP hybrid made from 3-APTMS and cyclohexanone

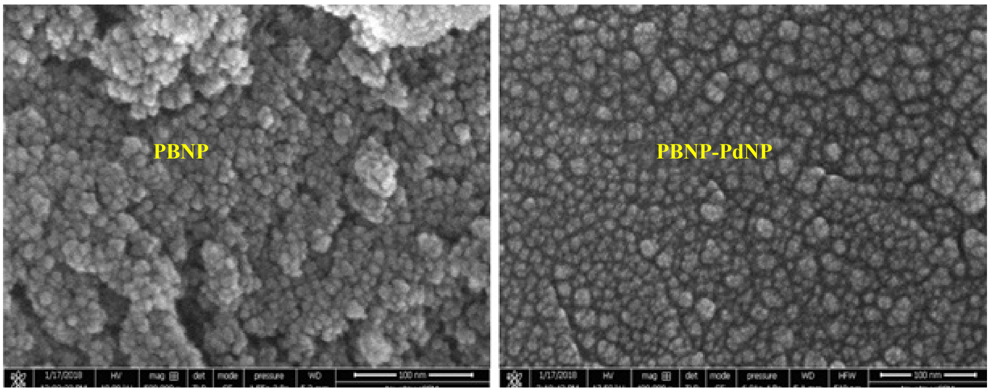

Figure 3b. HR SEM images of PBNP and PBNP-PdNP made from 2-(3, 4-epoxycyclohexyl) ethyltrimethoxysilane and tetrahydrofuran hydroperoxide

In order to further expand the contribution of these organic reagents we further attempted on simultaneous insertion of both PBNP and noble metal nanoparticles like PdNP within mesoporous silica nanoparticles. Such insertion of both PBNP and metal nanoparticles may allow to introduce several advances not only as vehicle for drug loan and deliver as reported earlier [25] but may allow a specific reaction to take place within mesoporous matrix and as generated reaction intermediate may undergo selective oxidation at electrode surface [30]. Indeed interesting findings on the synthetic insertion of these nanoparticles within mesoporous network of silica nanoparticles (MSNP) has been recorded. Figure 4a shows the TEM images of simultaneously inserted PBNP and PdNP within MSNP having pore size to the order of 6-7 nm. Figure 4b show the HR SEM and EDX of simultaneously inserted PBNP and PdNP within MSNP and clearly justify that these reagent allow synthetic insertion of both PBNP and metal nanoparticles within mesoporous architecture for specific application. Such finding provide novelty on using organic moieties/reagent that only allow selective insertion of metal nanoparticles along with PBNP within mesoporous matrix which is difficult to achieve either through electrodeposition or other techniques incorporating double precursors methods. The selective applications of such as made porous nanopmaterials are underway and will be reported in due course.

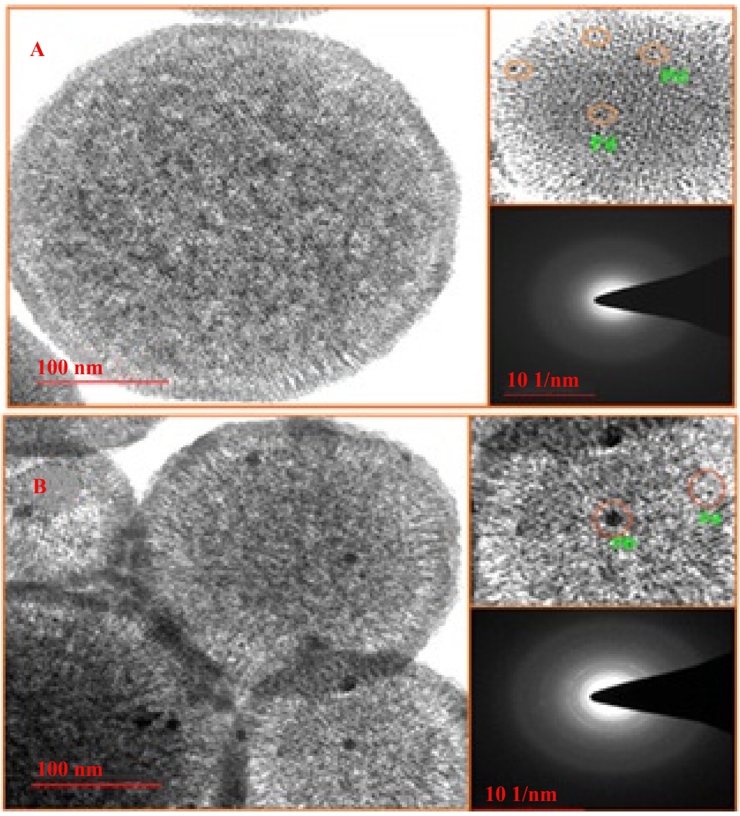

Figure 4a. TEM and SAED pattern of PdNPs (A) and simultaneously synthesized Pd-PBNPs (B), inserted within mesoporous silica nanoparticles

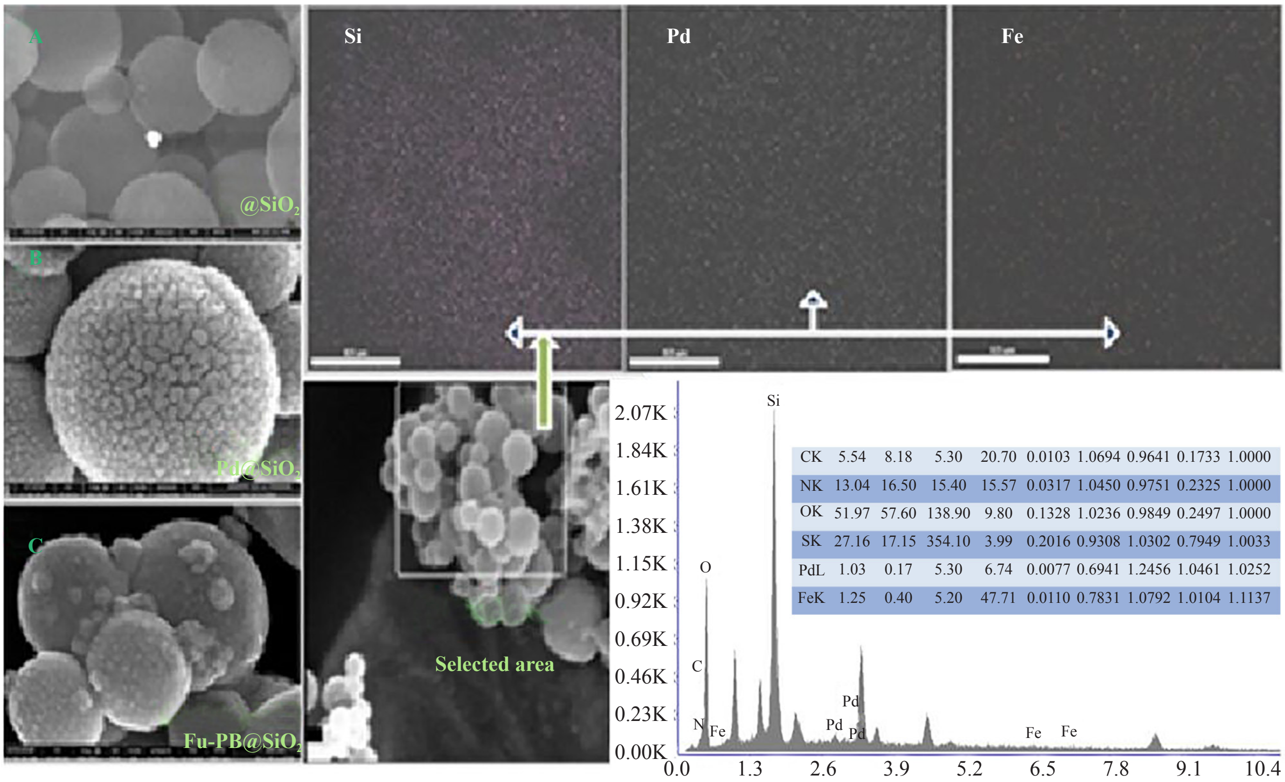

CK	5.54	8.18	5.30	20.70	0.0103	1.0694	0.9641	0.1733	1.0000
NK	13.04	16.50	15.40	15.57	0.0317	1.0450	0.9751	0.2325	1.0000
OK	51.97	57.60	138.90	9.80	0.1328	1.0236	0.9849	0.2497	1.0000
SK	27.16	17.15	354.10	3.99	0.2016	0.9308	1.0302	0.7949	1.0033
PdL	1.03	0.17	5.30	6.74	0.0077	0.6941	1.2456	1.0461	1.0252
FeK	1.25	0.40	5.20	47.71	0.0110	0.7831	1.0792	1.0104	1.1137

Figure 4b. HRSEM images of SiO2 (A), Pd@SiO2 (B), and PP-PB@SiO2 (C). Mapping analysis and EDX shows the presence of Fe, Pd element on silica nanoparticle

3.2 *Electrochemistry of PBNPs and PBNP hybrids*

After justifying the role of organic reagents in the synthesis of PBNP$_1$, PBNP$_2$, PBNP$_3$ and PBNP$_4$ and PBNP hybrids, it is important to examine the variation in electrochemical properties of these nanomaterials since two reversible redox couples corresponding to the oxidation of Prussian white (PW) and reduction of Prussian blue (PB) at (0.2 V), and another (0.9 V) owing to Prussian blue (PB) oxidation and reduction to Berlin green (BG) with potassium ion as the counter ion have been already very well established. Fiure 5a show redox electrochemistry of four type of PBNPs, i.e. PBNP$_1^-$, PBNP2$^-$, PBNP$_3^-$nd PBNP$_4^-$ modified electrode in 0.1 M KCl at the scan rate of 10 mV/s. The results clearly predict variable redox electrochemistry as a function of nanogeometry. The Electrochemical behavior of PBNP$_1$ and PBNP$_4$ are much better as compared to that of PBNP$_2$ and PBNP$_3$. Infact the finding based on voltammograms clearly demonstrate the existence of both reversible redox couples reflecting the role of organic moieties that relatively affect the reversibility of redox couples from ideal behavior normally recorded in j reducing agent however the size of PdNP$_2$ was found smaller as compared to that of PdNP$_1$ [31]. Apart from PdNP, AuNP and AgNP are important metal nanoparticles for further exploration. Subsequently the finding on the performance of PBNP-AgNP is evaluated on the elecrocatalytic reduction of hydrogen peroxide. Figure 5b show cyclic voltammofgrams of PBNP, PBNP-AgNP in absence (i) and after the presence of 1mM hydrogen peroxide (ii). The findings clearly predicts the followings; (1) the presence AgNP improve the redox activity of PBNP [Figure 5b (i)], (ii) the catalytic activity of PBNP-AgNP is much better on selective reduction of hydrogen peroxide as compared to that of only PBNP [Figure 5b (ii)]. The sensitivity of analysis is recorded in table 1 revealing the dependence of the same on the nanogeometry of PBNPs. These conclusion has further been supported from the amperometric measurement made at constant potential of 0.05 V vs Ag/AgCl [Figure 5b (iii)] along with calibration curve for cathodic sensing of hydrogen peroxide at the surface of PBNP-AgNP hybrid modified electrode.

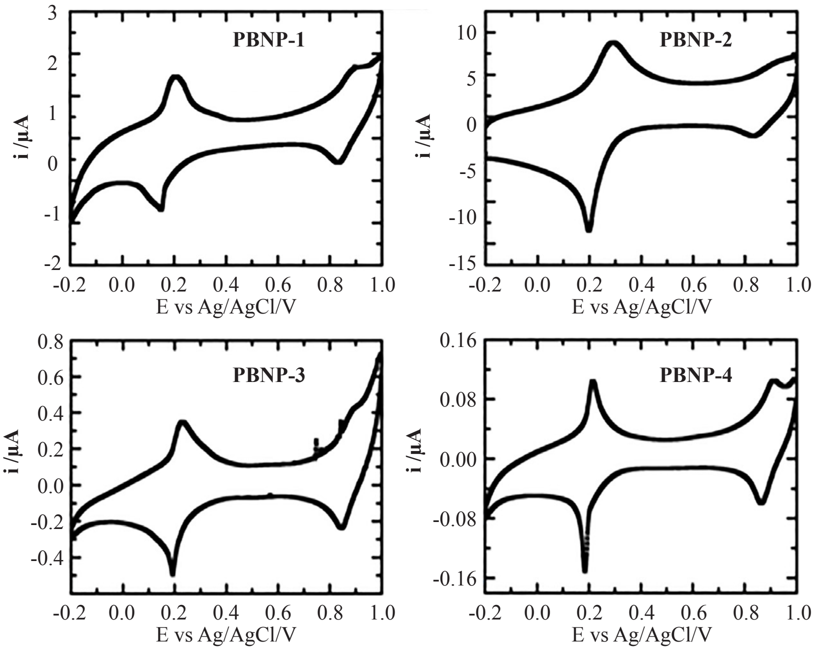

Figure 5a. Cyclic voltammograms of PBNP1, PBNP2, PBNP3 and PBNP4 in 0.1 M KCl at the scan rate of 10 mV/s

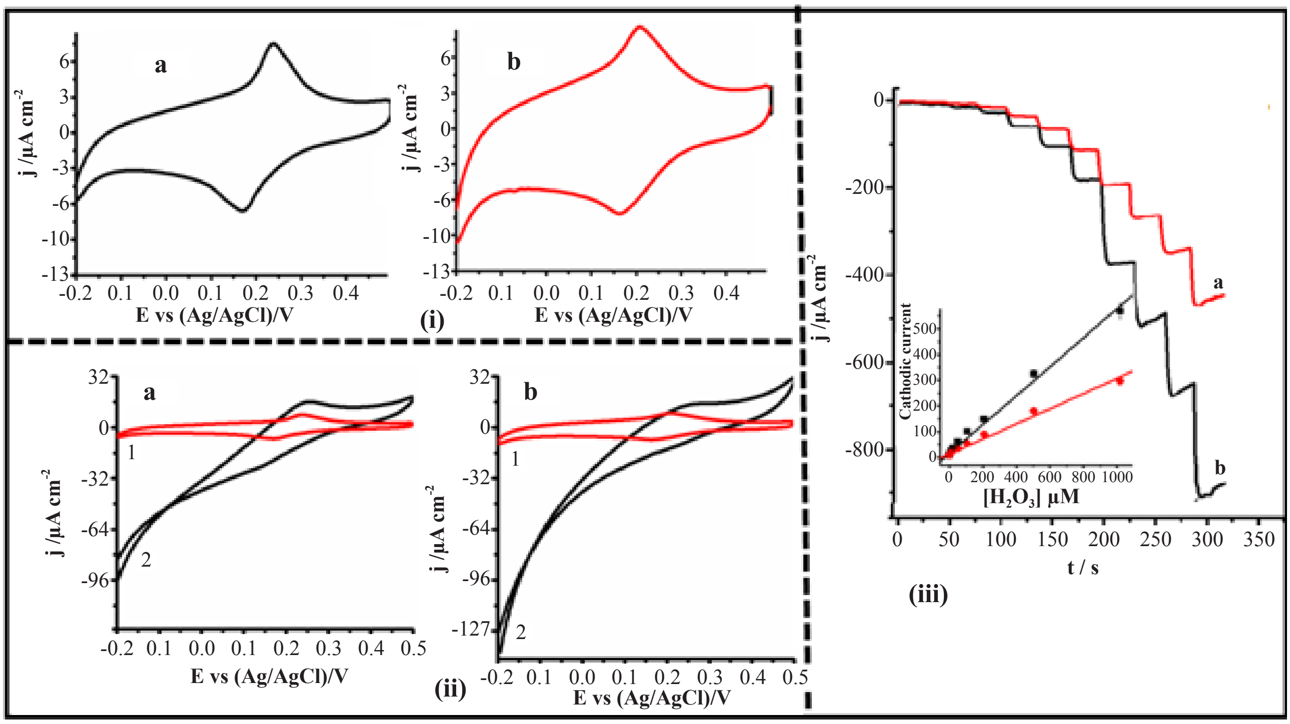

Figure 5b. (I) Cyclic voltammograms of PBNP (a) and PBNP-AgNP (b) modified electrode; (II) Cyclic voltammograms of PBNP (a) and PBNP-AgNP (b) modified electrode in absence (1) and the presence (2) of 5 mM hydrogen peroxide; (III) Amperometric responses of PBNP, PBNP-AgNP modified electrodes at 0.05 V vs AgCl on the addition of varying concentrations of hydrogen peroxide 0.1 M phosphate buffer pH-7.0 containing 0.1 M KC

Table 1. Organic reducing agent mediated formation of various metal nanoparticles and their property

Type of Nanomaterials	*Organic reducing agents mediated formation of Prussian blue from single precursor, potassium hexacyanoferrate*	*Electrocatalytic performance for H_2O_2 reduction/sensitivity of analysis/µA mM^{-1} cm^{-2}*	*Advantage of organic reducing agent mediated formation of Noble metal nanoparticles*	*Size of Prussian Blue nanoparticles (nm)*
PBNP-1	3-APTMS[=] and cyclohexanone	480	AuNP, AgNP, PdNP, Pd-Au/ Pd-Ag, Au-Pd/Ag	7-10
PBNP-2	Tetrahydrofuran hydroperoxide	330	AuNP, PdNP, Pd-Au/Au-Pd	40-50
PBNP-3	Tetehydrofuran and hydrogen peroxide	350	Does not enable the reduction of noble metal cations	30-40
PBNP-4	Tetrahydrofuran hydroperoxide and EETMS[==]	400	AuNP, PdNP, Au-Pd	8-15

*3-APTMS = #-Aminopropyltrimethoxysilane

**EETMS = [2-(3,4-Epoxycyclohexyl) ethyl] trimethoxysilane

We subsequently studied the PBNP hybrid formation between PBNPs and AuNP in presence and absence of other important functional materials like ruthenium bipyridyl (Rubpy) since Rupby is photoactive material and the hybrid of the same with PBNP may establish excellent photoelectrochemical significance. Figure 5c shows the electrochemical behavior of PBNP, PBNP-AuNP, PBNP-Rubpy and PBNP-Rubpy-AuNP modified electrodes. These hybrid materials display inherent electrochemical behavior of PBNP in the presence of these functional material and could be explored in specific applications. It is to be noted the presence of AuNP along with PBNP in the hybrid affect the both redox couples of PB. Nevertheless, the PB electrochemistry remains analogous to maximum extent in PBNP hybrid and need to be evaluated through electrocatalytic evaluation based on hydrogen peroxide sensing.

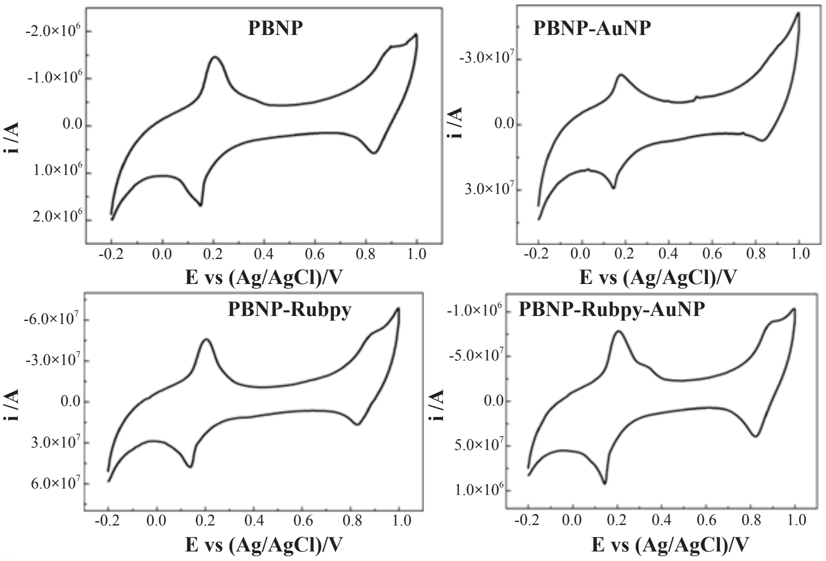

Figure 5c. Cyclic voltammograms of PBNP, PBNP-AuNP, PBNP-Rubpy, PBNP-Rubpy-AuNP in 0.1 M KCl at scan rate of 10 mV/s

3.3 *Glucose biosensing based on PBNPs and PBNP hybrid modified electrodes*

The PBNP is commonly designated as peroxidase mimetic. However the catalytic properties of the same should be tuned similar to that of peroxidase based on their turn over numbers. Nevertheless, we have been working on evaluating the peroxidase mimetic activity using hydrogen peroxide as natural substrate to precisely establish the comparative catalytic performance of peroxidase and PBNPs.

Hydrogen peroxide does not undergo mediated electrochemical interaction accordingly hydrogen peroxide may be electrochemically evaluated through catalytic reduction/oxidation of the same. Hydrogen peroxide undergo selective PBNP mediated reduction at lower potential accordingly the same could electrochemically detected based on the measurement of cathodic current (Figure 5b). The specific activity of horseradish peroxidase (HRP) has been found much better accordingly HRP has been selectively explored in electrochemical sensing of hydrogen peroxide. On the other hand, hydrogen peroxide also undergo oxidation at relatively high anodic potential and the dynamics of same is faster compared to that of H_2O_2 reduction as reported earlier [33]. Accordingly anodic current could be explored during hydrogen peroxide sensing with much better sensitivity however, the oxidation of same involve relatively large overvoltage and proceed close to 1.0 V vs AgCl at efficient measurable rate. If the overvoltage is reduced significantly, more sensitive electrochemical sensing could be desirable. Further the catalytic activity of Prussian blue could be precisely manipulated in the presence of other known electrocatalyst or functional material, the artificial catalytic system replacing natural enzyme. All oxidases catalyzed reactions allow the formation of hydrogen peroxide and electrochemical sensing of the same may only be realized via electocatalysis and not by mediated mechanism. Further, under anaerobic condition the redox centre of the oxidase enzyme may be regenerated either through the mediated mechanism [34-35] or through redox electrocatalysis [36]. Accordingly the PBNP hybrid electrode may serve as electrocatalyst as reported earlier [37] for both hydrogen peroxide and reduced oxidase enzyme that directed to probe glucose oxidase catalyzed reaction based on electrochemical biosensing using the PBNP hybrid electrode made with AuNP and Rubpy. The GOD along with PBNP and its hybrid was incorporated within graphite paste and the formation of hydrogen peroxide/reduced glucose oxisase as a function of glucose oxidase catalyzed reaction was monitored. Figure 5d show the cyclic voltammograms of PBNP-GOD, PBNP-AuNP-GOD, PBNP-Rubpy-GOD and PBNP-Rubpy-AuNP-GOD modified electrodes in absence (1) and the presence (2) of 200 mM glucose. The results clearly predict introduction of electrocatalysis in PBNP-Rubpy-AuNP-GOD during glucose biosensing. Such observation is further confirmed from the results sas hown in Figure 5e based on amperometric glucose biosensing as shown in Figure 5e PBNP-Rubpy-AuNP-GOD system showed much better electrochemical signal as compared to that of other three systems and predicted the introduction of electrocatalysis during redox enzyme based glucose biosensing. It is noteworthy to discuss the mechanism of glucose biosensing at the surface of PBNP-GOD hybrid modified electrode based on anodic current measurement. In fact hydrogen peroxide may be generated based on the availability of oxygen at the site of reaction as a function of glucose oxidase catalyzed reaction. Accordingly the electrocatalytic oxidation of as generated hydrogen peroxide was performed at 0.6 V vs Ag/AgCl and the sensitivity of electrochemical sensing will ultimately depend on the electrocatalytic efficiency of hybrid material derived from PBNP. Apart from little difference in electrocatalytic sensing of glucose oxidase catalyzed reaction involving only PBNP-PBNP-AuNP and PBNP-Rubpy nanohybrid modified electrode, the behavour of PBNP-AuNP-Rubpy system responded exceptionally well as compared to other three systems. The reason behind this may be predicted from the consideration of following bioelectrochemical reaction;

$$\text{Glucose} + \text{GOD[FAD]} \rightarrow \text{Gluconolactone} + \text{GOD[FADH}_2]$$

$$\text{GOD[FADH}_2] + [\text{Ru(bpy)}_3]^{3+} \rightarrow \text{GOD[FAD]} + [\text{Ru(bpy)}_3]^{2+}$$

$$[\text{Ru(bpy)}_3]^{2+} \xrightarrow[\text{Electrode}]{\text{HCF/HCF-AuNP/HCF-AuNPs-Rubpy}} [\text{Ru(bpy)}_3]^{3+} + e^-$$

Scheme 1. Mechanism of Rubpy mediated bioelectrochemical reaction

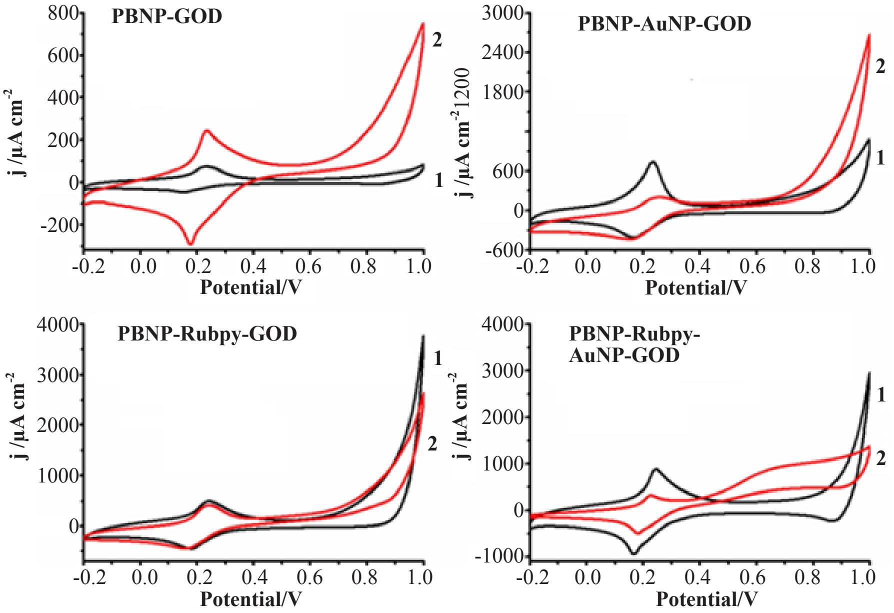

Figure 5d. Cyclic voltammograms of PBNP-GOD, PBNP-AuNP-GOD, PBNP-Rubpy-GOD, PBNP Rubpy-AuNP-GOD modified electrodes in absence (1) and the presence (2) of 200 mM glucose in 0.1 M phosphate buffer pH-7.0 containing 0.1 M KCl at the scan rate of 10 mV/s

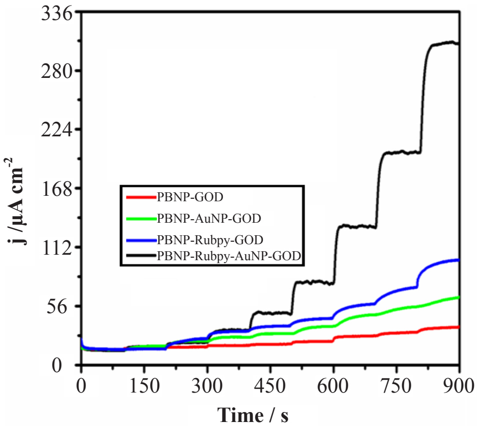

Figure 5e. Amperometric responses of PBNP-GOD, PBNP-AuNP-GOD, PBNP-Rubpy-GOD, PBNP-Rubpy-AuNP-GOD modified electrodes at 0.6 V vs AgCl on the addition of varying concentrations of glucose in 0.1 M phosphate buffer pH-7.0 containing 0.1 M KCl

It is to be noted that fraction of glucose oxidase may also undergo Rubpy mediated regeneration as shown in scheme-1 that may be regenerated electrochemically at 0.6V vs Ag/AgCl depending on electrocatalytic ability of PBNP hybrid electrode. We are working in details on such system and detailed output would be available in due course.

3.4 *Homogeneous catalysis of PBNP and PBNP hybrid as peroxidase mimetic*

The advantages of organic reagents can further be evaluated from the processability of as made PBNP useful as homogeneous catalyst involving o-dianisidine-H_2O_2 system. The catalytic mechanism involves the PBNP mediated catalysis of the two electron reduction of H_2O_2 to H_2O to form an intermediate complex; the colour substrate binds to the complex by a nucleophilic attack, thus allowing the oxidation reaction to occur with a colour change from colourless o-dianisidine to brown coloured product that can be monitored spectrophotometrically at 430 nm (Figure 6 a for PBNP and Figure 6b for PBNP-AuNP). Typical Michaelis-Menten curves can be obtained for the nanodispersion of PBNPs, PBNP-AuNP with H_2O_2 as substrates shown in Figure 6a and d respectively. The results recorded in Figure 6 clearly predict the use of PBNP as homogeneous catalyst and the catalytic activity may further be tailored by making nanohybrid of the same with metal nanoparticles.

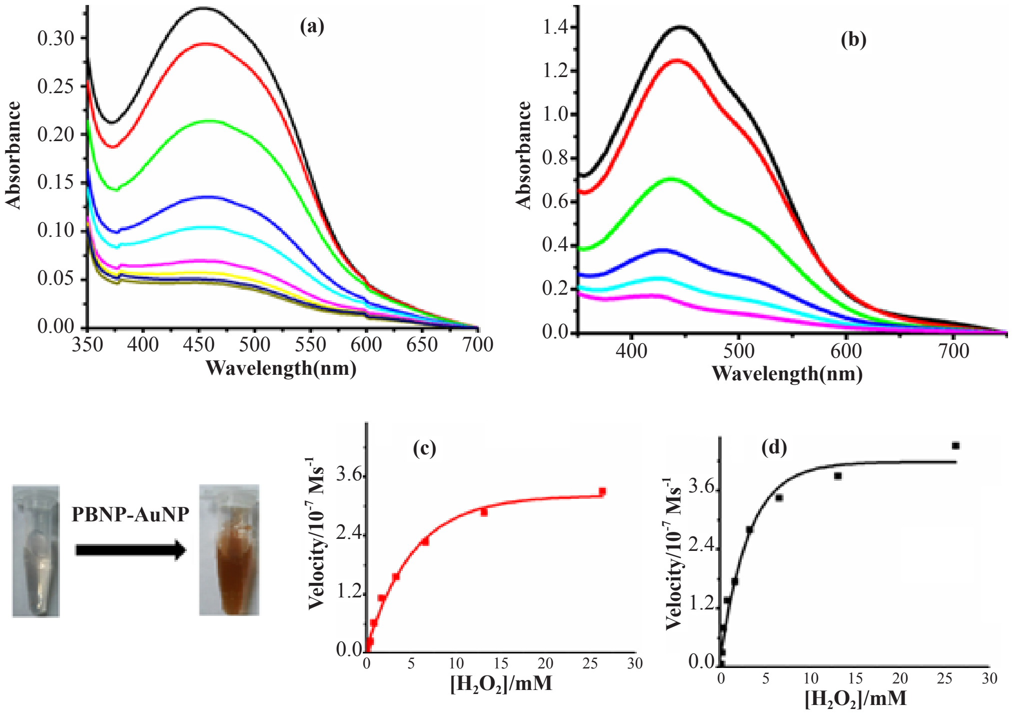

Figure 6. UV-Vis spectra of o-dianisidine-H_2O_2 system on the addition of PBNP (a) and PBNP-AuNP (b) with various concentrations of H_2O_2 (0.1, 0.2, 0.4, 0.8, 1.61, 3.23, 6.46, 25.84, 51.67 x 10^{-3}); Kinetic analysis of PBNP (c), and PBNP-AuNP (d) system with H_2O_2 as substrate. The inset show the visual image on the formation of coloured reaction product

4. Conclusion

In summary, we have demonstrated the role of four different organic systems; (1) 3-APTMS and cyclohexanone, (2) tetrahydrofuran hydroperoxide, (3) tetrahydrofuran hydrogen peroxide and (4) 2-(3, 4-epoxycyclohexyl) ethyltrimethoxysilane and tetrahydrofuran hydroperoxide in making four different types of PBNPs i.e. $PBNP_1$, $PBNP_2$, $PBNP_3$ and $PBNP_4$. These organic systems also enable the formation of monmetallic and bimetallic nanoparticles that can be further explored in making PBNP hybrids in order to tune the electrocatalytic activity for specific application. In addition these reagents also enable synthetic incorporation of both PBNP and metal nanoparticles especially PdNP within mesoporous network of silica nanoparticles or other similar materials for innovating PB based designs.

Acknowledgments

Thanks to DRDO for the financial support (Grant no. LSRB-316). CIFC, IIT (BHU) is highly acknowledged for TEM, SEM analysis.

References

[1] E. V. Karpova, A. A. Karyakin. Noninvasive monitoring of diabetes and hypoxia by wearable flow-through biosensors. *Current Opinion in Electrochemistry*. 2020; 23: 16-20.

[2] M. A. Komkova, E. E. Karyakina, A. A. Karyakin. Noiseless performance of prussian blue based (Bio) sensors through power generation. *Anal. Chem.* 2017; 89: 6290-6294.

[3] J. Cattermull, S. Wheeler[b], K. Hurlbutt[b], M. Pasta, A. L. Goodwin. Filling vacancies in a prussian blue analogue using mechanochemical post-synthetic modification. *Chem. Commun*. 2020. Available from: doi:10.1039/D0CC02922J.

[4] E. Ruiz, A. Rodríguez Fortea, S. Alvarez, M. Verdaguer. Is it possible to get high TC magnets with Prussian blue analogues? A theoretical prospect. *Chem. Eur. J*. 2005; 11: 2135-2144.

[5] T. Arun, K. Prakash, R. Kuppusamy, R. J. Joseyphus. Magnetic properties of Prussian blue modified Fe_3O_4 nanocubes. *J. Phys. Chem. Solids*. 2013; 74: 1761-1768.

[6] P. Varshney, M. Deepa, S. A. Agnihotry, K. C. Ho. Photo-polymerized films of lithium ion conducting solid polymer electrolyte for electrochromic windows (ECWs) Sol. *Energy Mater. Sol. Cells*. 2003; 79: 449-458.

[7] D. Ellis, M. Eckhoff, V. D. Neff. Electrochromism in the mixed-valence hexacyanides. 1. Voltammetric and spectral studies of the oxidation and reduction of thin films of Prussian blue. *J. Phys. Chem*. 1981; 85: 1225-1231.

[8] M. Pyrasch, B. Tieke. Electro-and photoresponsive films of Prussian blue prepared upon multiple sequential adsorption. *Langmuir*. 2001; 17: 7706-7709.

[9] K. Itaya, N. Shoji, I. Uchida. Catalysis of the reduction of molecular oxygen to water at Prussian blue modified electrodes. *J. Am. Chem. Soc*. 1984; 106: 3423-3429.

[10] R. Mažeikienė, G. Niaura, A. Malinauskas. Electrocatalytic reduction of hydrogen peroxide at Prussian blue modified electrode: An in situ Raman spectroelectrochemical study. *J. Electroanal. Chem*. 2011; 660: 140-146.

[11] G. Zhao, J. J. Feng, Q. L. Zhang, S. P. Li, H. Y. Chen. Synthesis and characterization of Prussian blue modified magnetite nanoparticles and its application to the electrocatalytic reduction of H_2O_2. *Chem. Mater*. 2005; 17: 3154-3159.

[12] J. Zeng, W. Wei, X. Liu, Y. Wang, G. Luo. A simple method to fabricate a Prussian Blue nanoparticles/carbon nanotubes/poly (1, 2-diaminobenzene) based glucose biosensor. *Mikrochim. Acta*. 2008; 160: 261-267.

[13] T. Kawamoto, H. Tanaka, M. Kurihara, M. Sakamoto, A. Oomura, H. Watanabe, A. Goto. US Patent 20110268963 A1. 2011.

[14] A. Gotoh, H. Uchida, M. Ishizaki, T. Satoh, S. Kaga, S. Okamoto, M. Tokumoto. Simple synthesis of three primary colour nanoparticle inks of Prussian blue and its analogues. *Nanotechnology*. 2007; 18: 345609.

[15] P. C Pandey. Indian Patent 295327. 2012.

[16] K. Itaya, T. Ataka, S. Toshima. Spectroelectrochemistry and electrochemical preparation method of Prussian blue modified electrodes. Spectroelectrochemistry and electrochemical preparation method of Prussian blue modified electrodes. *J. Am. Chem. Soc*. 1982; 104: 4767-4772.

[17] H. J. Lee, W. Cho, M. Oh. Advanced fabrication of metal-organic frameworks: template-directed formation of polystyrene@ZIF-8 core-shell and hollow ZIF-8 microspheres. *Chem. Commun*. 2012; 48: 221.

[18] G Maurin-Pasturel, J. Long, Yannick Guari, F Godiard, MarcGeorg Willinger, C. Guerin, J. Larionova. Nano-sized Au@Prussian Blue Analogues Heterostructures : Towards Multifunctionality at the Nanoscale. *Angew. Chem. Int. Ed*. 2014; 53: 3872-3876.

[19] P. C. Pandey, D. S. Chauhan. 3-Glycidoxypropyltrimethoxysilane mediated in situ synthesis of noble metal nanoparticles: Application to hydrogen peroxide sensing. *Analyst*. 2012; 137: 376-385.

[20] P. C. Pandey, R. Singh. Controlled synthesis of Pd and Pd-Au nanoparticles: effect of organic amine and silanol groups on morphology and polycrystallinity of nanomaterials. *RSC Adv*. 2015; 5: 10964-10973.

[21] P. C. Pandey, G. Pandey. One-pot two-step rapid synthesis of 3-aminopropyltrimethoxysilane-mediated highly catalytic Ag@(PdAu) trimetallic nanoparticles. *Catal. Sci. Technol*. 2016; 6: 3911-3917.

[22] P. C. Pandey, S. Shukla. Solvent dependent fabrication of bifunctional nanoparticles and nanostructured thin films by self assembly of organosilanes. *J. Sol-Gel Sci. Technol*. 2018; 86: 650-663.

[23] A. Bordage, R. Moulin, E. Fonda, G. Fornasieri, E. Riviere, A. Bleuzen. Evidence of the core-shell structure of (photo)magnetic CoFe Prussian blue analog nanoparticles and peculiar behavior of the surface species. *J. Am. Chem. Soc.* 2018. Available from: doi:10.1021/jacs.8b06147.

[24] Fornasieri, G., Bordage, A., Bleuzen, A. Magnetism and photomagnetism of Prussian blue analogue nanoparticles embedded in porous metal oxide ordered nanostructures eur. *J. Inorg. Chem*. 2018; 3-4: 259.

[25] P. C Pandey, G. Pandey, R. J. Narayan. Polyethylenimine-mediated synthetic insertion of gold nanoparticles into mesoporous silica nanoparticles for drug loading and biocatalysis. *Biointerfaces*. 2017; 12: 12. Available from: https://doi.org/10.1116/1.4979200.

[26] P. C. Pandey, A. K. Pandey. Cyclohexanone and 3-aminopropyltrimethoxysilane mediated controlled synthesis of mixed nickel-iron hexacyanoferrate nanosol for selective sensing of glutathione and hydrogen peroxide. *Analyst*. 2013; 138: 952-959.

[27] P. C. Pandey, A. K. Pandey. Novel synthesis of Prussian blue nanoparticles and nanocomposite sol: Electro-analytical application in hydrogen peroxide sensing. *Electrochim. Acta*. 2013; 87: 1-8.

[28] P. C. Pandey, A. K. Pandey. Tetrahydrofuran hydroperoxide mediated synthesis of Prussian blue nanoparticles: a study of their electrocatalytic activity and intrinsic peroxidase-like behavior. *Electrochim. Acta*. 2014; 125: 465-

472.
[29] P. C. Pandey, D. Panday. Tetrahydrofuran and hydrogen peroxide mediated conversion of potassium hexacyanoferrate into PBNPs: Application to hydrogen peroxide sensing. *Electrochim. Acta*. 2016; 190: 758-765.
[30] P. C. Pandey, S. Singh, S. N. Sawant. Functional alkoxysilane mediated controlled synthesis of Prussian blue nanoparticles, enabling silica alginate bead development; nanomaterial for selective electrochemical sensing.*Electrochim. Acta*. 2018. Available from: https://doi.org/10.1016/j.electacta.2018.05.003.
[31] P. C. Pandey, S. Singh, A. Walcarius. Palladium-Prussian blue nanoparticles; as homogeneous and heterogeneous electrocatalysts. *J. Electroanal. Chem*. 2018; 823: 747-754.
[32] P. C. Pandey, S. Singh, A. K Pandey. Tetrahydrofuran hydroperoxide and 3-Aminopropyltrimethoxysilane mediated controlled synthesis of Pd, Pd-Au, Au-Pd nanoparticles: Role of Palladium nanoparticles on the redox electrochemistry of ferrocene monocarboxylic acid. *Electrochim. Acta*. 2014; 138: 163-173.
[33] P. C. Pandey, S. Upadhyay, I. Tiwari, V. S. Tripathi. Ormosil-based peroxide biosensor-a comparative study on direct electron transport from horseradish peroxidase. *Sensors and Actuators B Chemical*. 2001; 72(3): 224-232.
[34] P. C. Pandey. Amperometric flow injection analysis biosensor for glucose based on graphite paste modified with tetracyanoquinodimethane. U. S. Patent 5, 378, 332. 1995.
[35] P. C. Pandey, H H Weetall. Application of photochemical reaction in electrochemical detection of DNA Intercalation.*Anal. Chem*. 1994; 66: 1236-1241.
[36] P. C. Pandey, C. Tran-Minh, F. Lantreibecq. Electrochemical Studies on Tetrathiafulvalene-Tetracyanoquinodimethane modified Acetylcholine/Choline sensor. *Appl. Biochem. Biotech*. 1991; 31: 145-158.
[37] P. C. Pandey, B. Singh. Library of Electrocatalytic sites in nanostructured domain. *Biosensors & Bioelectronics*. 2008; 24: 848-858.